Process Safety and Environmental Protection 207 (2026) 108353

Contents lists available at ScienceDirect

Process Safety and Environmental Protection

journal homepage: www.journals.elsevier.com/process-safety-and-environmental-protection

Generation and Decomposition of Reactive Oxygen and Nitrogen Species (RONS) in an Experimental Plasma Reactor for Wastewater Treatment

J.I. Quintana-Terriza [a,b,*], P. García-Muñoz [a], M.J. Mena [a], M. Zúñiga [a], C. Fernández García [b], J. Rodríguez-Chueca [a,**]

[a] Department of Industrial Chemical & Environmental Engineering, Escuela Técnica Superior de Ingenieros Industriales, Universidad Politécnica de Madrid, José Gutiérrez Abascal 2, Madrid 28006, Spain

[b] Technology Department, Cedrion, Consultoría Técnica e Ingeniería S.L, Leganés 28919, Spain

ARTICLE INFO

Keywords:
Plasma activated water (PAW)
Reactive oxygen nitrogen species (RONS)
Disinfection, decontamination
Disinfection by-products (DBPs)
Transient spark discharge

ABSTRACT

This study evaluates reactive species generation in two transient spark plasma reactors producing plasma-activated water from deionized water, tap water, and simulated wastewater. Plasma was applied above the liquid surface using a high-voltage source, and physicochemical changes were monitored during treatment and over two weeks post-treatment. Reactive species (nitrate, nitrite, ammonium, ozone, and hydrogen peroxide) were quantified, and tetracycline and *Enterococcus faecalis* were targeted. Complete pollutant removal was achieved in the 200 mL reactor across all water matrices, whereas the 1000 mL reactor required longer treatment times and exhibited reduced efficiency with wastewater. In the 200 mL reactor, energy efficiency per order was higher; ozone and hydrogen peroxide reached up to 1.5 ppm and 8 ppm, respectively; nitrate stabilized after 15 min, nitrite showed transient behavior, and ammonium increased continuously. The larger reactor exhibited similar but slower trends. Over two weeks, in both reactors, nitrate and ammonium remained stable, while ozone and hydrogen peroxide decayed rapidly. Plasma exposure caused an initial pH drop and an increase in conductivity, which subsequently stabilized. These findings underscore the critical role of reactor volume and water composition in PAW chemistry, pollutant removal, and reactive species stability, confirming plasma treatment as a sustainable, by-product-free technology for water remediation.

1. Introduction

Overpopulation has had a direct impact on water resources. In recent years, these resources have become increasingly exploited and contain higher concentrations of contaminants compared to previous decades (United Nations Educational Scientific and Cultural Organization, 2021). Additionally, the exponential growth of urban populations has led to an increased volume of wastewater, highlighting the urgent need for improving purification processes. Owing to the overexploitation of freshwater sources, the regeneration of wastewater has emerged as a critical alternative to reduce the demand for natural water supplies.

However, regeneration of wastewater has challenges that may difficulty the complete implementation in all the sectors. The main complications are: (1) the generation of disinfection by-products (DBPs), which result from the interaction between disinfectants and organic matter (Qadafi et al., 2023; Postigo et al., 2021); (2) the incomplete removal of contaminants of emerging concern (CECs), which are recently identified pollutants detected in aquatic environments at low concentrations (μg/L–ng/L) and are only partially regulated, although regulatory attention is increasing (Nathanael et al., 2024); (3) the need to ensure that pathogens have been properly removed, and the water reach the minimum quality standards to prevent environmental and human harm. In Spain, the composition of regenerated wastewater for different uses like agriculture, industrial activities or recreational purposes is regulated with the Royal Decree 1085/2024 (Real Decreto 1085/2024, 2024), preceded for the regulation EU 2020/741 (REGULATION (EU), 2020).

DBPs pose significant health risks, including increased cancer incidence, reproductive disorders, and hepatic and renal damage (Kali et al., 2021; Lou et al., 2021; Benson et al., 2017; Kalita et al., 2024; Grellier

* Corresponding author at: Department of Industrial Chemical & Environmental Engineering, Escuela Técnica Superior de Ingenieros Industriales, Universidad Politécnica de Madrid, José Gutiérrez Abascal 2, Madrid 28006, Spain.
** Corresponding author.
E-mail addresses: ji.quintana.terriza@upm.es, j.quintana@cedrion.com (J.I. Quintana-Terriza), jorge.rodriguez.chueca@upm.es (J. Rodríguez-Chueca).

https://doi.org/10.1016/j.psep.2025.108353
Received 26 September 2025; Received in revised form 4 December 2025; Accepted 20 December 2025
Available online 22 December 2025

et al., 2015). The most common DBPs are chlorine-derived trihalomethanes (THMs), such as chloroform, bromodichloromethane, dibromochloromethane, and bromoform. Chloroform and several brominated THMs exhibit carcinogenic, mutagenic, and cytotoxic effects in experimental studies (Kalita et al., 2024; Grellier et al., 2015; Wang et al., 2025). THMs also pose environmental risks, as many of these species can be bioaccumulated along the trophic chain, affecting aquatic ecosystems. In Spain, THMs concentrations in treated effluents are not yet regulated; however, their discharge into hydraulic systems represents a health risk, since this water may subsequently be abstracted for human consumption. The maximum permissible concentration in drinking water after potabilization is 100 μg/L for the sum of all THMs (Real Decreto 3/2023, 2023). Other DBPs include haloacetic acids (HAAs), such as dichloroacetic acid (DCAA), trichloroacetic acid (TCAA), and bromochloroacetic acid (BCAA), which are primarily formed through reactions between chlorine and various organic pollutants. Several HAAs display genotoxic, cytotoxic, and carcinogenic effects, with DCAA and TCAA among the most potent (Grellier et al., 2015; Wang et al., 2025; Shi et al., 2024). Additional DBPs include cyanogen halides (formed from reactions involving nitrogen, chlorine, and organic matter), bromate (produced during ozonation), and other chlorine-based inorganic oxyhalides such as chlorite, chlorate, and perchlorate (Kali et al., 2021; Lou et al., 2021). Bromate is a recognized carcinogen and nephrotoxic (Benson et al., 2017). Chlorite and chlorate can affect red blood cells and thyroid function and are primarily formed during the oxidation of chlorine-based disinfectants (Benson et al., 2017; Wang et al., 2025). Nitrogenous DBPs can also be detected. They are mainly formed when disinfectants react with organic nitrogen in wastewater, during chloramination, and in other nitrogen-rich matrices. These compounds are often more cytotoxic than regulated THMs and HAAs, and some have been reported to be more carcinogenic to humans (Kimura and Ortega-Hernandez, 2019; Krasner et al., 2013; Bond et al., 2015).

CECs refer to a broad range of chemical and biological substances that may pose risks to human health and ecosystems. These substances are widespread throughout the water cycle and include pharmaceuticals and personal care products, endocrine-disrupting compounds, per- and polyfluoroalkyl substances (PFAS), nanomaterials, antibiotics (like tetracycline), industrial chemicals and byproducts, pesticides, herbicides, microplastics, cyanotoxins, and heavy metals (Postigo et al., 2021; Guerra-Rodríguez et al., 2023).

There are lots of dangerous microorganisms or parasites that can be a high risk for the water use. Among pathogen microorganisms can be of different types like bacteria, viruses, protozoa or parasites. Some of the most common bacteria in urban wastewaters are *Escherichia coli,* that can cause severe diarrhoea and kidney damage. *Salmonella spp.* which can cause typhoid fever, gastroenteritis and septicaemia. *Shigella spp,* that causes shigellosis (severe diarrhoea, often bloody). *Campylobacter jejuni,* which causes bacterial gastroenteritis or *Enterococcus faecalis,* which also causes gastroenteritis and is an indicator of faecal contamination (McCarthy et al., 2025; Smith and Grimason, 2003; Hao, 2003; Behruznia and Gordon, 2022; Jang et al., 2017). Some of the most found viruses are *Hepatitis A,* responsible of liver inflammation, *Rotavirus*, causing severe diarrhoea. Protozoa like *Cryptosporidium parvum* of parasite like *Taenia spp.*, are also common in wastewater (McCarthy et al., 2025; Hao, 2003).

Conventional sanitation methods such as chlorination often result in DBP formation (Qadafi et al., 2023; Postigo et al., 2021; Morrison et al., 2022). Other techniques, such as UV-C irradiation, offer limited post-treatment effects and cannot guarantee water potability; and may also contribute to DBP formation (Xu et al., 2021). A major challenge for modern water purification systems is the simultaneous removal of CECs and antibiotic resistance genes, effective disinfection, and minimization of harmful DBP production. One promising approach involves advanced oxidation processes (AOPs) (Pandis et al., 2022). Among them, non-thermal plasma technologies have emerged as effective AOPs due to its ability to generate highly reactive species capable of degrading persistent pollutants without the necessity of additional chemical reagents (Thirumdas et al., 2018).

Plasma state is achieved by applying high-voltage electric fields, allowing plasma discharges to be generated in various ways, making this a versatile technology (Rezaei et al., 2019; Perinban et al., 2019; Meropoulis and Aggelopoulos, 2023; Quintana-Terriza et al., 2025). Plasma treatments are effective through two primary mechanisms: (1) direct interaction of the plasma discharge with pollutants, leading to their decomposition; and (2) the formation of reactive species in the water due to gas molecule decomposition and recombination. Water treated through this method is referred to as plasma-activated water (PAW).

When air is used as the discharge gas, reactive oxygen and nitrogen species (RONS) are primarily formed, many of which possess high oxidative potential. These include short-lived species such as hydroxyl radicals ($^{\bullet}OH$) ($E^o = 2.8$ V), singlet oxygen ($^1O_2$) ($E^o = 2.42$ V), superoxide (O_2^-) ($E^o = 0.93$ V), and peroxynitrates ($ONOO^-$) ($E^o = 0.35$ V) (Andrés et al., 2023; Van Gils et al., 2013). Additionally, more stable species such as hydrogen peroxide (H_2O_2) ($E^o = 1.78$ V) and ozone (O_3) ($E^o = 2.07$ V) are also generated (Machala et al., 2013; Wong et al., 2023). Nitrogen-derived species tend to enter the water more slowly via diffusion and mainly exist in stable forms such as nitrate (NO_3^-), nitrite (NO_2^-), and ammonium (NH_4^+) (Rezaei et al., 2019; Perinban et al., 2019; Lee et al., 2021; Wang et al., 2022; Maniruzzaman et al., 2017; Khlyustova et al., 2019; Zhao et al., 2020). The generation of these reactive species alters the physicochemical properties of the water, reducing the pH, and increasing conductivity and oxidation-reduction potential (ORP) (Thirumdas et al., 2018; Zhao et al., 2020; Calvo et al., 2020; C. et al., 2015).

In this study, the evolution during treatment of the more stable species generated in the water (nitrates, nitrites, ammonium, ozone, and hydrogen peroxide) were analysed. One experimental plasma reactor based on transient spark discharge was used. Two different reactors volumes (200 and 1000 mL) and different aqueous matrices (deionized water (DW), tap water (TW), and simulated wastewater (SWW) were compared. While the pollutant removal efficiency changes due to the chemical variations was evaluated with *Enterococcus faecalis* as an indicator of faecal contamination in water and tetracycline as a CECs target. Lastly, the formation of organic and inorganic DBPs under each condition was assessed to determine the technology's capacity for efficient pollutant removal without harmful by-product formation. This work has focused on the limited information available on low-consumption transient spark plasma discharges. One main difference of the reactor used in this work was that it does not require an external gas flow to induce plasma discharge, unlike most current data (Rezaei et al., 2019; Machala et al., 2013; Bruggeman et al., 2016; Zhang et al., 2023; Zhong et al., 2023) Additionally, an extensive study comparing the influence of aqueous matrix effects was provided. Lastly, the scalability of this type of plasma reactor has not yet been extensively studied, as most recent literature focuses on a fixed volume (Rezaei et al., 2019; Panchal et al., 2024; Komarudin et al., 2023; Ma et al., 2020).

2. Methodology

2.1. Chemicals reagents

Throughout this work, various reagents were used. Meat peptone (CAS 91079–40–2), meat extract (CAS 68920–68–7), urea ($CO(NH_2)_2$, CAS 57–13–6, synthesis grade), NaCl (CAS 7647–14–5, synthesis grade), $CaCl_2{\cdot}2H_2O$ (CAS 10043–52–4, extra pure powder), $MgSO_4{\cdot}7H_2O$ (CAS 7487–88–9, extra pure), and K_2HPO_4 (CAS 7758–11–4, extra pure) were purchased from Scharlau. Slanetz-Bartley Medium ISO and Luria Broth (Miller's LB Broth) were obtained from Condalab. Sodium carbonate (anhydrous, CAS 497–19–8, for analysis ISO-ACS), sodium bicarbonate (CAS 144–55–8, for analysis ACS), and oxalic acid dihydrate (CAS 6153–56–6, for analysis ACS) were acquired from Carlo Erba Reagents.

Titanium (IV) oxysulfate solution (1.9–2.1 % for H_2O_2 determination, CAS 56391–06–1) was sourced from Supelco. Ultrapure pentane (CAS 109–66–0) was obtained from Sigma Aldrich. Nitrate, nitrite, ozone, ammonium and chemical oxygen demand (COD) reactive packs were obtained from Hanna Instruments.

2.2. Water preparation and experimental procedure

Three aqueous matrices were tested: deionized water (DW), tap water (TW), and simulated secondary wastewater (SWW). DW was purified using a PURELAB QUEST system (VEOLIA), ensuring removal of all dissolved ions and substances. TW was obtained from the laboratory tap and allowed to stand for 24 h to allow chlorine dissipation. This matrix contains higher concentrations of dissolved compounds compared to DW (details in Table S1 from Supplementary Material). SWW was prepared using tap water and the following composition per litre: 32 mg of meat peptone, 22 mg of meat extract, 6 mg of urea ($CO(NH_2)_2$), 7 mg of NaCl, 4 mg of $CaCl_2{\cdot}2H_2O$, 2 mg of $MgSO_4{\cdot}7H_2O$, and 28 mg of $K_2H_2PO_4$. This formulation simulates the composition of effluents after secondary treatment at a municipal wastewater treatment plant and was adapted from (Polo-López et al., 2012). Among the three matrices, SWW had the highest concentration of both inorganic and organic compounds, particularly total organic carbon. Full water composition and initial physicochemical characteristics are presented in Table S1. To assess pollutant removal efficiency, 25 ppm of tetracycline and 10^6 CFU/mL of *Enterococcus faecalis* were added to each matrix. Although these concentrations exceed those typically found in real wastewater, they were selected to facilitate precise laboratory analysis.

The preparation procedures for the two reactor volumes were similar. For 200 mL treatments, a 250 mL beaker was used, while a larger beaker of one litre was used for the 1000 mL treatments. Electrode supports were scaled accordingly for each reactor. Initially, each aqueous matrix was characterized (time 0). The beaker was then placed on a magnetic stirrer, filled with the tested matrix (DW, TW, or SWW), and subjected to plasma discharge for varying durations (15, 30, 45, and 60 min). After treatment, the discharge was stopped, and the water was immediately characterized. Aliquots were collected for the quantification of target reactive species, as will be described in Section 2.4. Each experiment was conducted by triplicate. Error bars have been calculated using Excel with a significance level of $\alpha = 0.05$ and following a T-student distribution. All the data have been represented with Origin.

2.3. Plasma system

Plasma discharge was generated using an experimental system previously described on (Quintana-Terriza et al., 2025). The reactor was designed to produce a low-consumption discharge between a high-voltage electrode positioned at the centre of the reactor and the liquid surface, which was connected to the low-voltage electrode. A vortex, created by a magnetic stirrer, maintained separation between the high-voltage electrode and the water surface. Both electrodes were made of tungsten doped with 0.5 % lanthanum and were mounted using a 3D-printed PLA (polylactic acid) support. This support was specifically designed to minimize condensation of evaporated water on its surface. Fig. 1A illustrate the scheme of the electrical discharge and Fig. 1B the support or the electrodes and the plasma discharge.

The distance between the high-voltage electrode and the water surface was maintained at approximately 8 mm, regulated via the vortex generated by external stirring. Plasma was produced using a high-voltage DC power supply (Heinzinger, 30 kV, 20 mA). Discharges were initiated when the applied voltage exceeded the breakdown threshold of 4 kV. The operating voltage ranged from 4 to 8 kV, with medium current of 4 mA. With a cycle time of 25 ms (40 Hz) resulting in an average power input of 23 W.

The plasma discharge has been considered as a transient spark, based on the literature (Bruggeman et al., 2016; Janda, 2011; Akishev et al., 2010) and due to the geometry of the electrodes, where the high voltage electrode had higher curvature in proportion to the collector electrode. The plasma discharge is produced on the tip of the needle as seen in Fig. 1B.

2.4. Physico-chemical characterization

Physical-chemical characterization of water samples was performed through different equipment. Parameters like pH, ORP and conductivity were measured using a Metrohm pH/conductometer model 914 with different probes (pH PT1000/B/2/3 M KCl from 0 to 14; ORP Pt/3 M KCl; conductivity Pt 1000/B). For organic and inorganic concentration carbon, a total organic carbon analyser Teledyne TOC-TORCH was used. While a multiparametric photometer, model HI83399 from Hannah Instruments was used for evaluating the chemical oxygen demand (COD), ammonium, nitrate, nitrite and ozone concentrations. For the hydrogen peroxide evaluation, the colorimetric method (Eisenberg,

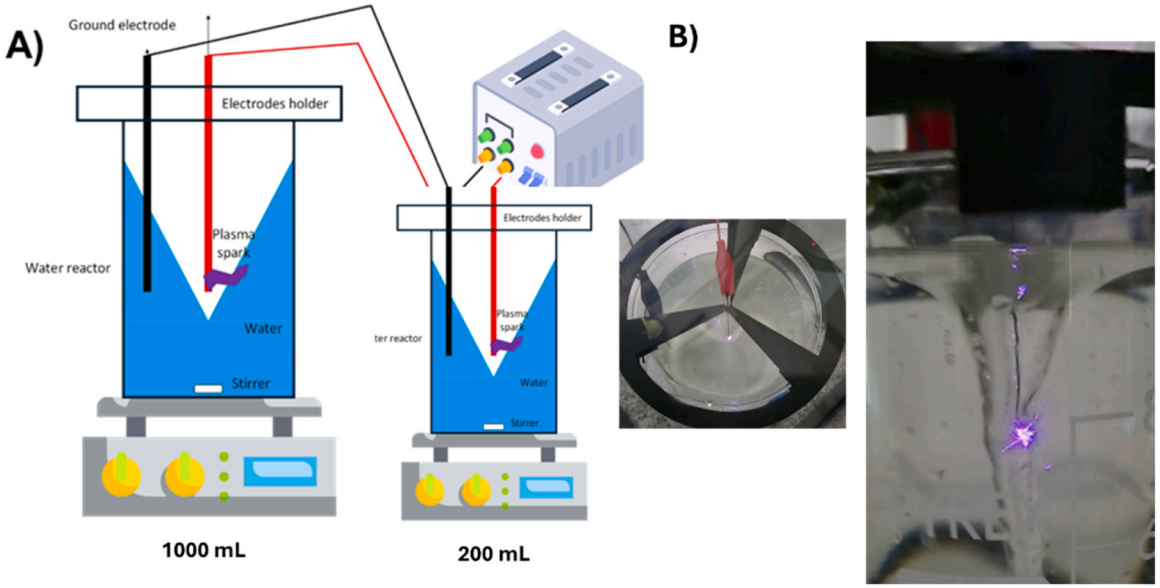

Fig. 1. Schematic representation of the experimental setup. voltage ranged 4–8 kV, current of 2–4.5 mA. Frequency of the plasma discharges of 40 Hz. Medium power of 23 Wh.

1943) of reaction with titanium (IV) oxysulfate was used. This method was based on the absorbance change at 407 nm in the solution after adding the titanium sulphate reagent. The absorbance was measured using a UV5 spectrophotometer from METTLER TOLEDO.

Inorganic DBPs were measured with ionic chromatography ECO IC from Metrohm, with 8 mM of sodium carbonate and 0.25 mM of sodium bicarbonate as eluent, in a flow rate of 0.7 mL/minute with a column Metrosep A Supp 19 250/4.0 and a precolumn Metrosep A Supp 19 Guard/4.0. THM were analysed with a gas chromatography mass spectrometer PerkinElmer Clarus 600 GC-MS, equipped with TurboMass software version 5.4.0. Following Method 6232 B 35 mL of the sample and 2 mL of pentane was added. After 1 min of mechanical shaking at 100 rpm the sample was injected in the GC column (30 m × 0.25 mm, 0.25μm, Elite-5MS, PerkinElmer). With a split ratio of 50 % and an injection volume of 0.25 μL, respectively. Helium was used as carrier. The oven, source and the inlet line temperatures were set at 200ºC. For the MS detection, selective ion recording (SIR) was employed targeting the *m/z* values of the specific THMs and their retention times. Table S2 (Supplementary Material) shows the different methods followed for chemical determinations in this study.

The different parameters were evaluated at time 0, 15, 30, 45 and 60 min during the activation time. And characterized 7 and 14 days after the activation to know the evolution of the different chemical species. The samples analysed for evolution where storage on a close flask at 4 ºC in a freezer. Before the characterization, the samples were left to reach environment temperature.

2.5. Microbiological procedure

Samples were inoculated with a commercial strain of *Enterococcus faecalis* (ATCC® 29212™). A fresh liquid culture was prepared by incubating *E. faecalis* in Luria-Bertani (LB) broth for 24 h at 37 °C under orbital shaking conditions. Following incubation, the bacterial suspension was harvested via centrifugation at 4500 rpm for 15 min. The resulting bacterial pellet was resuspended in sterile saline solution (0.9 % NaCl) and subsequently diluted in the experimental reactor to achieve an initial concentration of 10^6 CFU/mL.

Quantitative analysis of bacterial populations in the collected samples was performed using both the drop plate and spread plate methods after serial decimal dilutions in sterile saline solution (0.9 % NaCl). For the drop plate method, three aliquots of 10 μL from each dilution were plated onto Slanetz & Bartley Medium ISO agar. In the spread plate method, a 100 μL aliquot of each diluted sample was uniformly distributed on agar plates using sterile glass beads. Plates were incubated at 37 °C for 48 h, after the colony-forming units (CFUs) were enumerated. The detection limit (DL) for each experiment was determined using the spread plate method and was established at 10 CFU/mL.

2.6. Tetracycline measurement procedure

Tetracycline analysis was performed using a High-Performance Liquid Chromatography (HPLC) system (Agilent Series 1100). The chromatographic separation was achieved using a KromaPhase C18 precolumn (5 μm particle size, 100 Å pore size, 10 × 4 mm; Scharlau), connected in series to a KromaPhase C18 analytical column (5 μm particle size, 100 Å pore size, 150 × 4.6 mm; Scharlau). The mobile phase consisted of acetonitrile and 2 % acetic acid in a volumetric ratio of 15:85 (v/v). The flow rate was maintained at 1.0 mL/min, with an injection volume of 5 μL.

The tetracycline degradation was analysed as the Eq. (1), where C_0 is the initial tetracycline concentration, and C_t concentration at each time. This equation has been taken from (Meropoulis and Aggelopoulos, 2023).

$$D(\%) = \frac{C_0 - C_t}{C_0} \cdot 100 \quad (1)$$

2.7. Process energy efficiency

The energy efficiency is an important factor in plasma systems. For this reason, the energy efficiency of the plasma system was calculated in terms of energy per order (E_{E0}). That represents the amount of energy required for reducing the contaminant concentration in one order of magnitude (90 %) in 1 m^3 of water, this energy efficiency factor, has been obtained from (Triantaphyllidou and Aggelopoulos, 2025) and is defined in Eq. (2).

$$E_{E0} = \frac{P \quad (kW) \cdot t(h)}{V(m^3) \cdot \log(\frac{C_0}{C_t})} \quad (2)$$

Where "*P*" is the medium power consumption in kilowatts, "*t*" is the treatment time required for at least one order reduction in hours, "*V*" is the volume treated in cubic meters, "C_0" is the initial concentration and "*Ct*" is the concentration at the time required for one order reduction. This efficiency was used for comparing both the biological inactivation and tetracycline degradation.

3. Results and discussion

The results are presented in two main sections: first, the chemical comparison between reactors and water matrices in terms of species generation and evolution in plasma-activated water (PAW). Second, a comparative analysis of pollutant removal efficiency, including disinfection by-product (DBP) formation evaluation.

Unless stated otherwise, the data are represented using the following notation: DW (blue square), TW (red circle), and SWW (black triangle). Data from the 200 mL reactor are shown as dotted lines and hollow symbols; data from the 1000 mL reactor are shown as continuous lines and filled symbols. Pseudo–first-order kinetic constants for species generation are listed in Table S3, Table S4 provides an extended list of PAW-related reactions and last Table S5 shows the calculation of the energy efficiencies, all of them in the supplementary material.

3.1. Physical characterization of PAW

Due to the plasma treatment an increase in the concentration of different species was generated in the PAW, inducing the change of physical parameters of the samples. Some of them, like the pH have a direct impact on the PAW reactivity, not only in the pollutant removal but also in the reactions that take place (Lukes et al., 2014; Naítali et al., 2010) as it will be discussed along the text. In Fig. 2A, the pH evolution shows a rapid decrease in the 200 mL reactor, reaching a pH of 3 withing 15 min for DW and SWW. In contrast, this decrease was slower in the TW matrix, requiring 30 min. This slower kinetics (Table S3) can be attributed to the presence of buffering substances, such as carbonates. Species like carbonates delay the pH reduction process induced due to the plasma treatment (Papalexopoulou et al., 2025). In the case of the 1000 mL reactor the pH reduction was lower, for DW, it was stabilized in pH 4 after 30 mins of treatment. For SWW there was a slight reduction to pH 5 and in the case of TW there was no significant reduction after 60 min of treatment. pH reduction is related with the increase in the nitrogen derived species (Machala et al., 2013; Lukes et al., 2014), as it will be discussed later, the nitrite and nitrate concentration increase with the treatment time, being responsible for the pH reduction.

The conductivity, shown in Fig. 2B, is directly related with the pH value. As some authors have previously reported (Ma et al., 2020; Naítali et al., 2010), a decrease in the pH is related to an increase in the electrical conductivity in the sample. In the 200 mL reactor, a rapid decrease in pH was observed, leading to an increase in the concentration of various dissolved species in the PAW. This is also reflected in the increased conductivity of the samples. There is not a significance difference between aqueous matrices. In the case of the 1000 mL reactor,

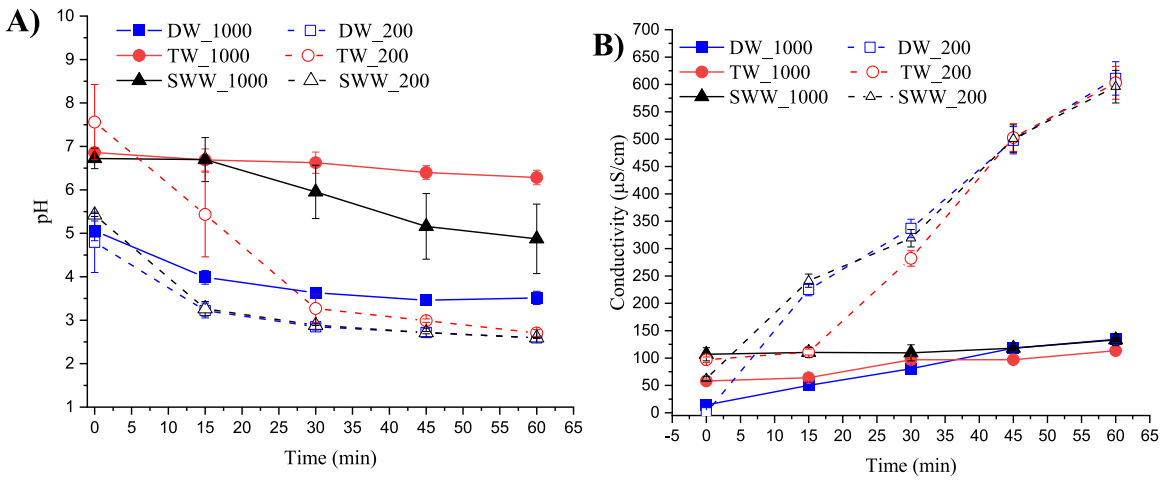

Fig. 2. Evolution during plasma activation. Reactor of 200 mL discontinuous line, reactor of 1000 mL continuous line. DW (blue), TW (red), SWW (black). A)pH. B) Conductivity (µS/cm).

the increase in the conductivity was lesser, with a lower kinetic rate mainly due to the less ratio plasma energy/volume (Table S3). Dissolved species in the PAW are directly related with the variations in the pH and conductivity values. It is known that higher values of nitrates reduce the pH values (Lukes et al., 2014; Bruggeman and Leys, 2009) and increase the conductivity (Figure S1 from supplementary material).

3.2. Chemical comparison between activation volumes in different reactors

Plasma treatment applied to the water, produce the generation of reactive species in the water. ROS will not only be generated in the water but also due to the interaction with the reactive species generated in the air. In the case of the nitrogen, reactive species generated in the water comes strictly from the nitrogen contained in the air (Machala et al., 2013; Lee et al., 2021; Wang et al., 2022). Nitrogen species present in the plasma air phase like N_2, NO_2, N_xO_x (Bruggeman et al., 2016; Bruggeman and Leys, 2009) diffuse inside the water producing NO_2 (aq) then, nitrogen species reacts in the water to generate nitrates and nitrites following the Eqs. (3–4) (Lukes et al., 2014).

$$NO_{2\ (aq)} + NO_{2\ (aq)} + H_2O_{(l)} \rightarrow NO_2^- + \quad NO_3^- + 2H^+ \tag{3}$$

$$NO_{(aq)} + NO_{2\ (aq)} + H_2O_{(l)} \rightarrow 2NO_2^- \quad + 2H^+ \tag{4}$$

The Fig. 3 presents the concentration changes of various chemical species over time during plasma treatment in two different volumes reactors. In Fig. 3A, the generation of nitrate is shown. In the case of the reactor of 200 mL, there was an increase of nitrate species during the first 15 min to reach a plateau for the rest of the treatment time in the different aqueous matrices. In the case of the 1000 mL reactor, the stationary phase of formation and consumption of the nitrate was not reached, being necessary longer treatment times for reaching the plateau than in the smaller reactor. This difference was mainly to the increase of the reactor volume, while the plasma discharge was in the same range. In both reactors the concentration of nitrate reached was higher in TW then SWW and lastly DW. This difference could be explained for the initial concentrations in the samples, while in TW and SWW there were some dissolved nitrates in DW there were any. It is also possible to see how in the case of the DW the plateau in the 1000 mL reactor was appearing near the minute 45/60. This required time for the reactor of 1000 mL was near 5 times more than the required time for the 200 mL reactor to reach the plateau. This additional required time will be seen along the discussion of the different species and pollutant removal and is mainly due to the increase of the volume of the reactor.

In Fig. 3B the nitrite generation in the reactor is shown. In this case there was a higher discrepancy between water matrixes. In the case of DW and the 200 mL reactor, it was seen that was produced for the first minutes, after 15 min of treatment it started to decompose, this effect is due to the Eq. (5) (Lukes et al., 2014; Anbar and Taube, 1954). The reaction rate of Eq. 5 is increased when the pH is reduced (Anbar and Taube, 1954). As seen in Fig. 2A, the pH for DW was reduced below 3 after 15 min of treatment, moment where the nitrite concentrations decompose (Wang et al., 2022). In the case of the nitrite generation in TW in the reactor of 200 mL a similar effect occurred but after 30 min, required time for a pH lower than 3 (Fig. 2A). For SWW the concentration of nitrite in the water entered in constant value after 15 min, moment when the pH was near 3. For the reactor of 1000 mL, the concentration of nitrite generated was near 100 times lower than in the 200 mL reactor, again due to the less ratio of energy per volume in this reactor. In this case, the Eq. 5 had importance mainly in DW, due to this was the only aqueous matrix in the 1000 mL reactor that achieve a pH lower than 3. In SWW and TW, as the pH was higher, the decomposition of nitrite was also lower, being the concentration of nitrite increased with a higher kinetic than DW (Table S3), and it was not produced the decomposition of the nitrite seen in the 200 mL reactor. Eq. 7 also participates in the consumption of the nitrite, as later will be discussed, but occurs in a much lower reaction rate than Eq. 5.

$$NO_2^- + \quad H_2O_2 + H^+ \rightarrow NO_3^- + \quad H_2O + H^+ \tag{5}$$

Water treated with plasma can also get enriched in ammonium. However, its formation from the nitrogen present in the water is more complex as it is required the reduction of the nitrogen from valence 6 + (NO_3^-) or 4 + (NO_2^-) to valence 3- (NH_4^+), following the Eqs. (6, 7), (Yang et al., 2021; Ren et al., 2015; Guo et al., 2015). In Fig. 3C, the ammonium production in the reactor is shown. As it can be seen the generation was slower but constant for all the conditions. The higher increase, in the case of the SWW, in comparation with DW and TW in both reactors, was due to the presence of the initial ammonium cation in different components of the SWW formulation (urea, meat extract, and meat peptone). However, most of the ammonium generated in SWW is coming from the urea hydrolyzation following the Eq. 8 (Schuchert-Shi and Hauser, 2008). In this reaction the generation of the ammonium was increased for an acid pH. The differences in ammonium production between the reactor of 200 mL and the 1000 mL were due to the pH difference (Fig. 2 A) while in the reactor of 200 mL was around 3 after 15 min, in the reactor of 1000 mL reactor was 5 after the 60 min of treatment.

$$NO_3^- + 8e^-_{(aq)} + 10 \quad H^+ \rightarrow NH_4^+ + 3H_2O \tag{6}$$

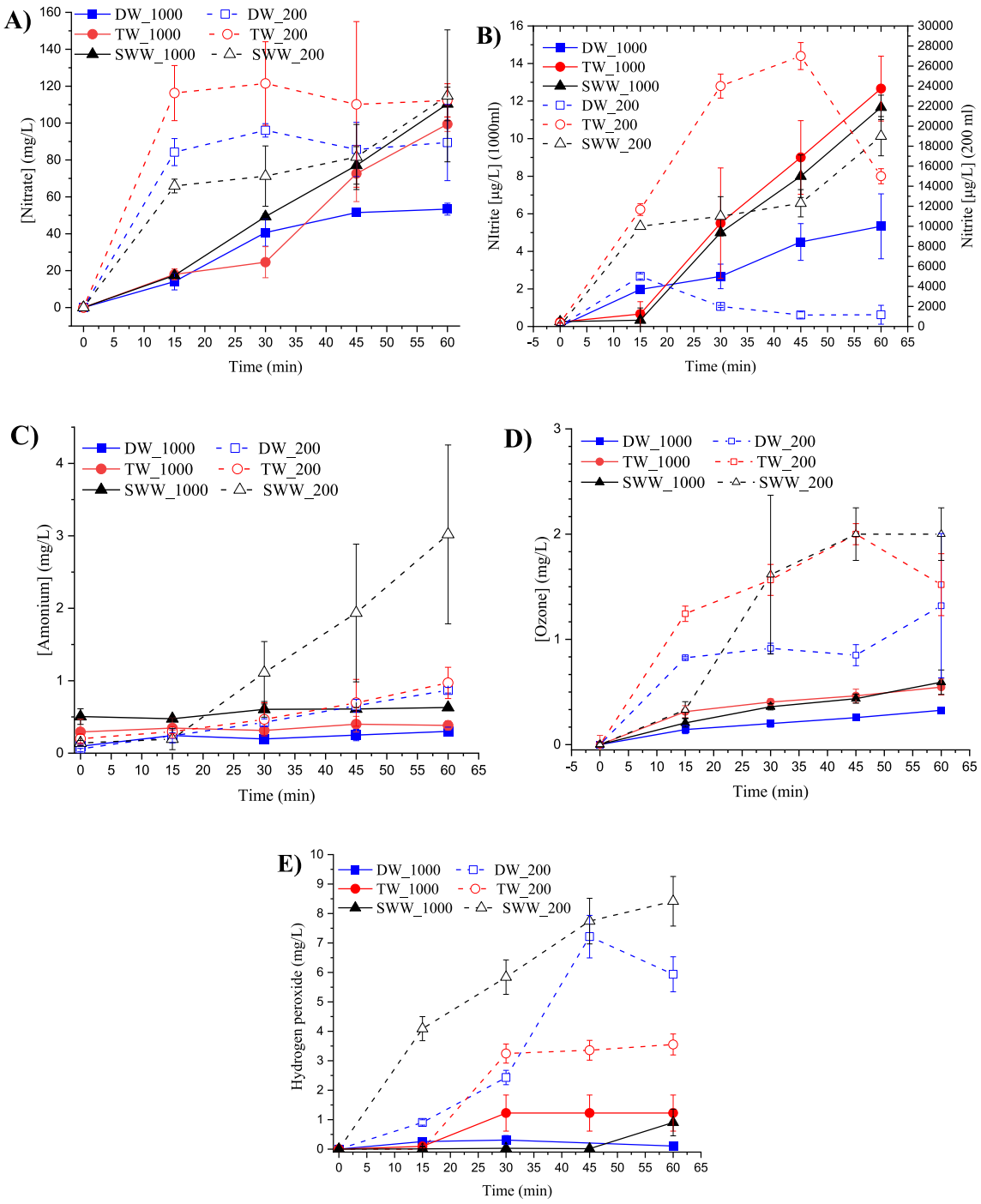

Fig. 3. Evolution of the main species analysed during plasma treatment. Reactor of 200 mL discontinuous line, reactor of 1000 mL continuous line. DW (blue), TW (red), SWW (black). A) Nitrate (mg/L). B) Nitrite (µg/L). C) Ammonium (mg/L). D) Ozone (mg/L). E) Hydrogen peroxide (mg/L).

$$NO_2^- + 6e^-_{(aq)} + 8\ \ H^+ \rightarrow NH_4^+ + 2H_2O \quad (7)$$

$$NH_2CONH_2 + \ \ H_2O + \ \ H^+ \rightarrow 2NH_4^+ + HCO_3^- \quad (8)$$

Plasma interaction with the water also generates oxygen reactive species. These ROS can be generated i) directly in water or ii) in air and then diffuse into water. This work focused on the study of more stable ROS like ozone and hydrogen peroxide dissolved on the bulk water. Fig. 3D illustrates the ozone concentration in both reactors along the treatment time. Based on the preliminary statement, the ozone was generated through two mains different vias, firstly, the ionization of the air generates it directly following Eqs. (9-10) (Amsalu et al., 2024), for later diffuse into the water. And secondly, it is possible to generate the ozone inside of the water due to reaction between short live reactive species derived from the oxygen, following the Eq. (11) (Lukes et al., 2014; Papalexopoulou et al., 2025). Ozone dissolved in the water, not only can act as a precursor of other RONS (Eqs. 12–14) (Papalexopoulou et al., 2025; Zoumpouli et al., 2020; Von Gunten, 2003) but also can react directly with organic material dissolved (Eqs. 15–16) (Papalexopoulou et al., 2025; Von Gunten, 2003) or some metallic cations present in the water (Eq. 17) (Wei et al., 2017). This reactivity was the reason for a low concentration in the reactor after treatment as will be discussed later. When working with 200 mL volume reactor the ozone

concentration was proportionally increased along the treatment time, having a higher generation rate at the first 30 min, for this point the decomposition and generation rates were similar. The equilibrium between formation and consumption of ozone in the DW, was mainly due to Eqs. (12–14), in the case of TW also had importance the Eq. (17) where previous authors have reported the influence of the metal cations in the decomposition of oxidant species (Papalexopoulou et al., 2025). In the reactor of 1000 mL, the reaction rates (shown in table S3) were much lower passing from values of 0.055 down to 0.005 mg/L and not achieving 0.5 mg/L after 60 min of treatment in any of the aqueous matrices due to the scaling of the reaction volume.

$$O_2 + e^- \rightarrow 2O + \quad e^- \tag{9}$$

$$2O + 2O_2 \rightarrow 2O_3 \tag{10}$$

$$O_{(aq)} + O_2 \quad _{(aq)} \rightarrow O_3 \quad _{(aq)} \tag{11}$$

$$O_3 \quad _{(aq)} + OH^- \rightarrow HO_2^- + O^2 \tag{12}$$

$$O_3 \quad _{(aq)} + HO_2^- \rightarrow \quad \bullet OH + \quad O_2^- + O^2 \tag{13}$$

$$O_3 \quad _{(aq)} + O_2^- \rightarrow \quad O_3^- + O^2 \tag{14}$$

$$O_3 \quad + \quad OM_1 \rightarrow OM_{1(ox)} \tag{15}$$

$$O_3 \quad + \quad OM_2 \rightarrow OM_2^+ + O_3^- \tag{16}$$

$$O_3 \quad + \quad Fe^{2+} \rightarrow Fe^{3+} + O_3^- \tag{17}$$

Besides, in Fig. 3E, the evolution of hydrogen peroxide in both reactors is also shown. Once again, the H_2O_2 generated in the 200 mL reactor (maximum values near 7 mg/L) was again higher than in case of the 1000 mL reactor (maximum values near 1 mg/L). This can be explained due to the fact that the same source of energy was employed and so the energy/volume ratio was diminished. The low-rate formation of hydrogen peroxide was related with the high reactivity of the molecule with the rest of the components in the PAW. Hydrogen peroxide was mainly produced following the Eqs. (18, 19) (Kooshki et al., 2024; Rocha et al., 2025). The Eq. (19) can occur either in gas state or in liquid phase. Hydrogen peroxide has a high reduction potential (E^0 = 1.76 V), reacting quickly with other components form the PAW, some reactions had already been discussed, like in Eq. (5). But also, can experience a similar reaction process with organic matter than ozone (Kooshki et al., 2024) (Eqs. 15–16), or being induced a Fenton effect in the presence of metallic anions like Fe (Kooshki et al., 2024). Lastly the mutual reaction between hydrogen peroxide and ozone Eq. (20) (Zhang et al., 2025) known as peroxone reaction can produce hydroxyl radicals capable of high degradation rates. Hydrogen peroxide is also decomposed into water by thermal decomposition.

$$2H_2O \rightarrow H_2O_2 + 2H^+ + 2e^- \tag{18}$$

$$\bullet OH_{(g,aq)} + \bullet OH_{(g,aq)} \rightarrow H_2O_2 \tag{19}$$

$$O_3 + H_2O_2 \rightarrow H_2O + \quad O_2 + \bullet OH \tag{20}$$

Table 1 compiles information on the characterization of chemical species carried out in studies conducted by other authors. As it can be seen, in the final chemical composition of the PAW, there are some variables that exert a more notable influence, like the gas ionized, the type of the water or the type of plasma employed. For instance, technologies where argon or oxygen are ionized, higher concentration of oxygen derived species are produced (Meropoulis and Aggelopoulos, 2023; Papalexopoulou et al., 2025) and less of nitrogen derived species, while air produced lower rates of ROS and higher concentration of nitrogen species than argon plasmas. Additionally, technologies based on dielectric barrier discharge (DBD) or plasma bubbles induced higher

Table 1
Recopilation of chemical species characterized in other works.

Plasma system	Treatment time	Volume treated	Solution	pH	Gas	H_2O_2	NO_2^-	NO_3^-	O_3	NH_4^+	Units	Ref
Pulsed discharge			Phosphate buffer	3.30	O_2/N_2	0.20	0.09	0.13			mmol/L	(Lukes et al., 2014)
Pulsed discharge			Phosphate buffer	6.90	O_2/N_2	0.21	0.10	0.14			mmol/L	(Lukes et al., 2014)
Microjet	20 min	20 mL		4.50	air		21.00	37.00			ppm	(Liu et al., 2010)
Micropulsed plasma bubbles	20 min		DW	3.0	air	1.50		200.00	1.75		mg/L	(Papalexopoulou et al., 2025)
Micropulsed plasma bubbles	20 min		TW	7.50	air	0.50		175.00	0.10		mg/L	(Papalexopoulou et al., 2025)
gas-liquid DBD	20 min		DW	1.50	O_2/air	420.00		1650.00	15.00		mg/L	(Papalexopoulou et al., 2025)
Plasma microbubles	20 min		DW	6.20	air	2.00	0.50	25.00	0.15		mg/L	(Meropoulis and Aggelopoulos, 2023)
gas-liquid DBD	20 min		DW	3.50	AIR	23.00	3.00	275.00	1.00		mg/L	(Meropoulis and Aggelopoulos, 2023)
DBD-Cu electrode	30 min		TW	3.10		0.10	17.00				mg/L	(Kooshki et al., 2024)
DBD-Ce electrode	30 min		TW	3.10		15.00	2.00				mg/L	(Kooshki et al., 2024)
Plasma jet	1 min	0.1 mL	DW	4.0	argon		$8.00 \cdot 10^{-6}$	$1.00 \cdot 10^{-4}$	$2.9 \cdot 10^{-6}$		mol/L	(Van Gils et al., 2013)
Plasma jet	15		TW		Air	8.70	10.00	23.00			Ppm	(Ma et al., 2017)
Plasma jet	15		TW		Nitrogen	1.70	2.50	0.15			ppm	(Ma et al., 2017)
Pulsed plasma	60 min	200	DW	2.60	air	2.50	1.17	89.45	1.32	0.87	ppm	This work
Pulsed plasma	60 min	200	TW	2.70	air	3.30	15.00	112.30	1.53	0.97	ppm	This work
Pulsed plasma	60 min	200	SWW	2.60	air	7.74	19.00	114.75	2.00	3.02	ppm	This work
Pulsed plasma	60 min	1000	DW	3.50	air	0.11	5.33	53.35	0.32	0.30	ppm	This work
Pulsed plasma	60 min	1000	TW	6.40	air	0.00	12.66	99.40	0.54	0.38	ppm	This work
Pulsed plasma	60 min	1000	SWW	4.80	air	0.91	11.67	110.40	0.59	0.63	ppm	This work

concentrations of oxygen derived species than other technologies based in the generation of the plasma discharge above the water surface, like spark or pulsed discharge which produce higher concentration of nitrogen derived species.

3.3. Physicochemical evolution of water composition after plasma treatment

After analysing the species generated during the treatment time, the evolution of them through two weeks was studied. Physicochemical values are constant after the treatment as it is shown in Figure S2 (Supplementary Material). Previous studies (Lukes et al., 2014) had demonstrated that PAW does not have a significant change in the

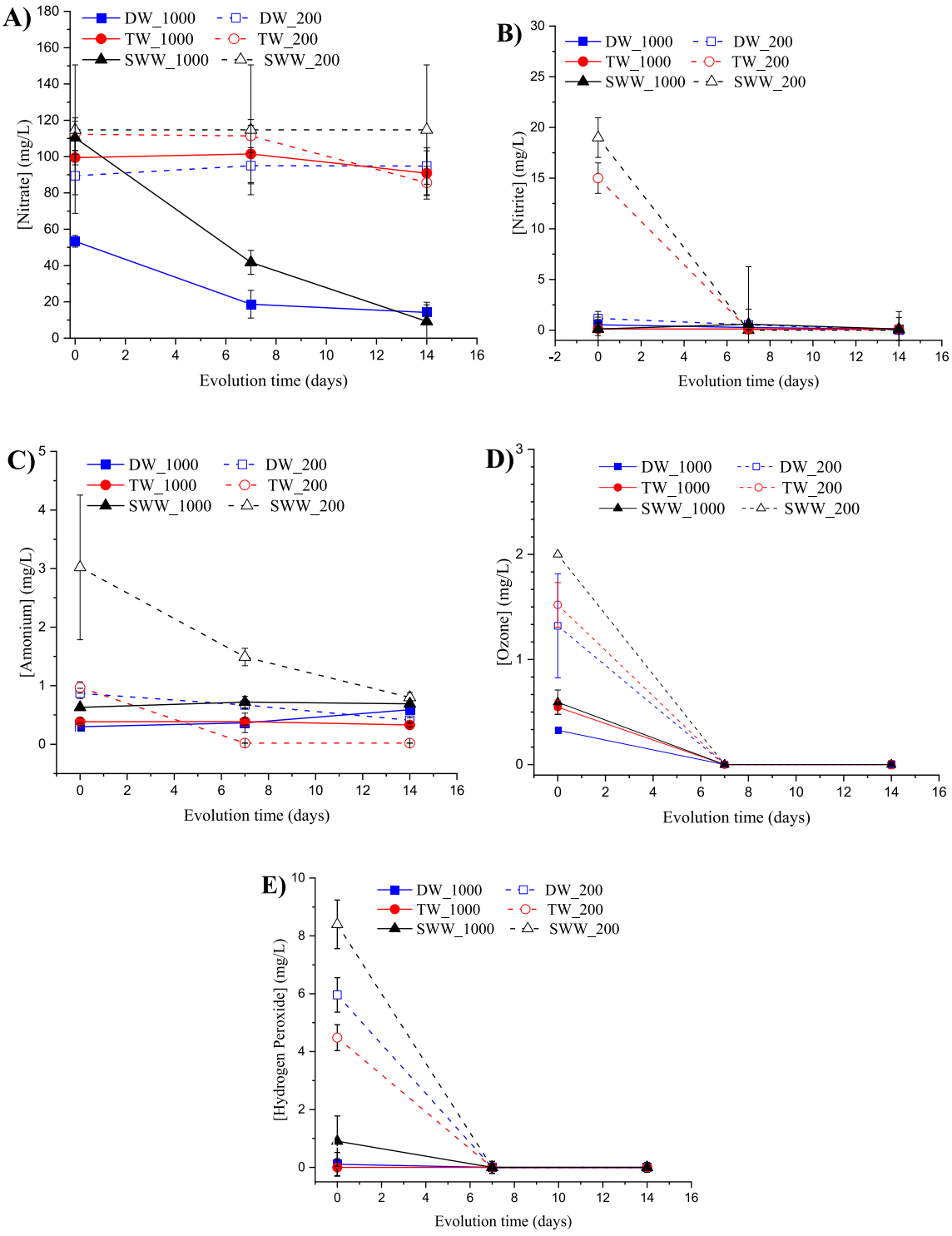

Fig. 4. Evolution after activation for two weeks. Reactor of 200 mL discontinuous line, reactor of 1000 mL continuous line. DW (blue), TW (red), SWW (black). A) Nitrate (mg/L). B) Nitrite (mg/L). C) Ozone (mg/L). D) Ammonium (mg/L); E) Hydrogen peroxide (mg/L).

physicochemical properties. However, it can be a variation in the water composition and in the concentrations of the different species during the first minutes after the treatment (Lukes et al., 2014). The stability of the pH was mainly produced for the generation of nitrogen acidic species which are stable, like nitrates dissolved in the water (Machala et al., 2013; Lukes et al., 2014). Besides, the pH stability is also responsible for the conductivity constant value (Thirumdas et al., 2018).

In Fig. 4 the evolution of every analysed specie is shown. In the case of the nitrate Fig. 4A, the concentration remained stable for most of the samples treated in the 200 mL reactor. Previous studies (Lukes et al., 2014) have reported similar results where the nitrate concentration was usually stable, while nitrite concentration was reduced along the time to nitrate. In the 1000 mL reactor, TW displayed similar behaviour to the analogous of 200 mL reactor, but for those cases of SWW and DW, there was a reduction in more of the half of the concentration after one week of the treatment and in the case of the SWW, was even lower two weeks later. It has not been possible to find a proper explanation for the reduction of the nitrate concentration under these circumstances. However, some possible justifications have been theorized but require further analysis for confirmation. I) Biological process of denitrification where some bacteria in presence of organic or inorganic carbon can reduce nitrate to nitrogen in absence of oxygen. Some of these bacteria are *Pseudomonas stutzeri* or *Bacillus subtilis*, both can be in airborne state and do not suppose a risk for human health, being possible to be in the lab during the experimental sessions and enter in the water sample. This will mainly explain the reduction in the case of SWW. In the case of DW, as there is not carbon, the nitrification process would not happen, unless some carbon contamination of the sample or the reactor has occurred (Wang et al., 2024; Zumft, 1997). II) Reduction of the nitrate to nitrite or ammonium (in presence of organic matter), this process is the intermedium phases of the one described previously. However, the concentration of both species (nitrite and ammonium) was reduced during the post-treatment time as seen in Fig. 4 B, C (Wang et al., 2024; Zumft, 1997). III) Nitrate could be assimilated by some microorganisms to generate amino acids (Wang et al., 2024; Zumft, 1997).

The nitrite concentration was also reduced along the time in all the aqueous matrices and in different reactor volumes, mainly due to the Eq. (5). In the case of the TW in the 1000 mL reactor the nitrite concentration was not reduced due to neutral constant pH of the samples (Fig. 2A) and to the lack of hydrogen peroxide after the treatment (Fig. 4 E). The ammonium concentration during the post treatment time was constant, suggesting that it was a stable specie. Previous studies (Rezaei et al., 2019) showed a 75 % reduction of the nitrite concentration from the initial value after a few hours of treatment, and a reduction of more than 50 % in the hydrogen peroxide concentration while the nitrate was increased. This was correlated with the results obtained where in general the nitrite was reduced when the pH is acid while the nitrate was increased.

In the case of the oxygen derived species (Fig. 4 D, E), both had a similar tendency, and after one week there were not any specie detected. Despite that, in acidic pH, ozone shows higher lifetime than in neutral or basic pH. Normally, dissolved ozone slowly decomposes into oxygen with a half-life of 20–30 min (Van Gils et al., 2013; Khadre et al., 2001). Ozone in TW was also decomposed by reacting with metallic ions (Eq. 17), and in the case of SWW, the interaction with the organic material in water produces its depletion (Eqs. (15–16)). The hydrogen peroxide had a similar reactivity; it reacts and oxidize fast with the species contained in water.

3.4. Pollutant removal efficiency

Pollutant removal efficiency is based on two main factors, on one side the direct interaction of plasma with the main pollutant and on the other side by the reaction of the species generated by plasma (Van Gils et al., 2013). From the species and parameters analysed in this work, the main ones that participate in the degradation of the pollutants, usually are ozone, hydrogen peroxide, and the short time reactive species generated during the discharge like hydroxyl radical, singlet oxygen, peroxynitrates (Machala et al., 2013; Wang et al., 2022; Khlyustova et al., 2019) among others. Additionally, the pH has a key role in the degradation and the chemical species generation rates (Wang et al., 2022). However, short time reactive species have not been measured in this work .

In Fig. 5 the pollutant removal efficiency is depicted. For *E. faecalis* inactivation, in the 200 mL reactor, short treatments times were needed for reaching at least 5 log reductions, 5 min, 20 min and 10 mins for DW Fig. 5A, TW Fig. 5B and SWW Fig. 5C, respectively, when *E. faecalis* was the unique pollutant in the aqueous matrix. The required time was increased in most of the aqueous matrices with the 1000 mL reactor, requiring 40 min and 20 min for DW and TW. For SWW, no reduction was observed in the 1000 mL reactor. The changes between reactors were related to the lower generation rate of reactive species for higher volumes (kinetics shown in Table S3), and the smaller concentration of ozone (0.5 mg/L in the 1000 mL reactor and 1.25 mg/L in the 200 mL reactor) and hydrogen peroxide as previously discussed. In the case of the TW there were no difference between reactors, mainly associated to the presence of low concentration residual chloride (Table S1, Supplementary Material). The residual chlorine in the presence of the plasma can generate reactive chlorine radicals and hypochlorite radicals (Anbar, 1964). Some authors (Papalexopoulou et al., 2025) have remarked the enhance that those species produce to the inactivation of bacteria and in the pollutant degradation. The increase in the treatment time can be also related to the higher pH measured in the 1000 mL reactor. Authors like Ikawa et al. (Ikawa et al., 2010) have reported that pH must be lower of 4.7 for bactericide effects. Additionally, Ikawa et al. study obtains 6 logarithmical reductions in 3 min in a volume of 500 μL, supposing a linear scalability, would be required more than 2 h of treatment (this estimation is make only having in consideration the treatment times and volumes). Ma et al. (Ma et al., 2017) achieved 5 logarithmical reductions of *E. coli* in near 35 min on air jets, while using nitrogen jets there is not a significance reduction observed after 50 min, suggesting that the ROS generated have a key role in bacteria inactivation. Van Gils et al. (Van Gils et al., 2013) achieve 6 reductions in 120 s in a volume of 100 μL with an air plasma jet. The energy efficiency per order in previous works is much higher than the obtained in this works, calculated in the Table S5. The efficiency for only *E. faecalis* in the reactor of 200 mL was 2.14 kW/m^3 while in the 1000 mL was 7.5 kW/m^3.

When tetracycline was added to the reactors (green lines in Fig. 5A, B and C), the treatment times to achieve complete inactivation of *E. faecalis* was increased. In the reactor of 200 mL, for DW was required 25 additional minutes of treatment for reaching the same reduction percentage and in the case of SWW 20 additional minutes were needed. For TW, a similar behaviour was obtained needing the same time, due to the presence of residual chloride, as previously discussed. Something similar occurs with the energy efficiency per order, where the addition of the tetracycline in the system increased the E_{EO} to 35 kW/m^3 for DW. For the reactor of 1000 mL in case of DW and TW the treatment time was the same than in case of treating a single contaminant, however as the volume was larger the efficiency was better in the 1000 mL reactor with an efficiency of 7.1 kW/m^3 for DW. For SWW, no reduction in 1 h were reached. The increase in the reaction time between the presence of one or more contaminants and the reduction in the energetic efficiency per order reduction (from 2.14 kW/m^3 for DW when there is only *E. faecalis* to 7.5 kW/m^3 when there are both contaminants in the reactor of 200 mL) suggested that there was a competition of the reactive species between contaminants. Being reduced the depletion efficiency with concurrent pollutants in water. This hypothesis was also confirmed with the treatment of the samples of SWW. While it was possible to achieve 5 log reductions in the *E. faecalis* concentration, there was any reduction reached when *E. faecalis* and tetracycline were dissolved in the sample for the 1000 mL reactor.

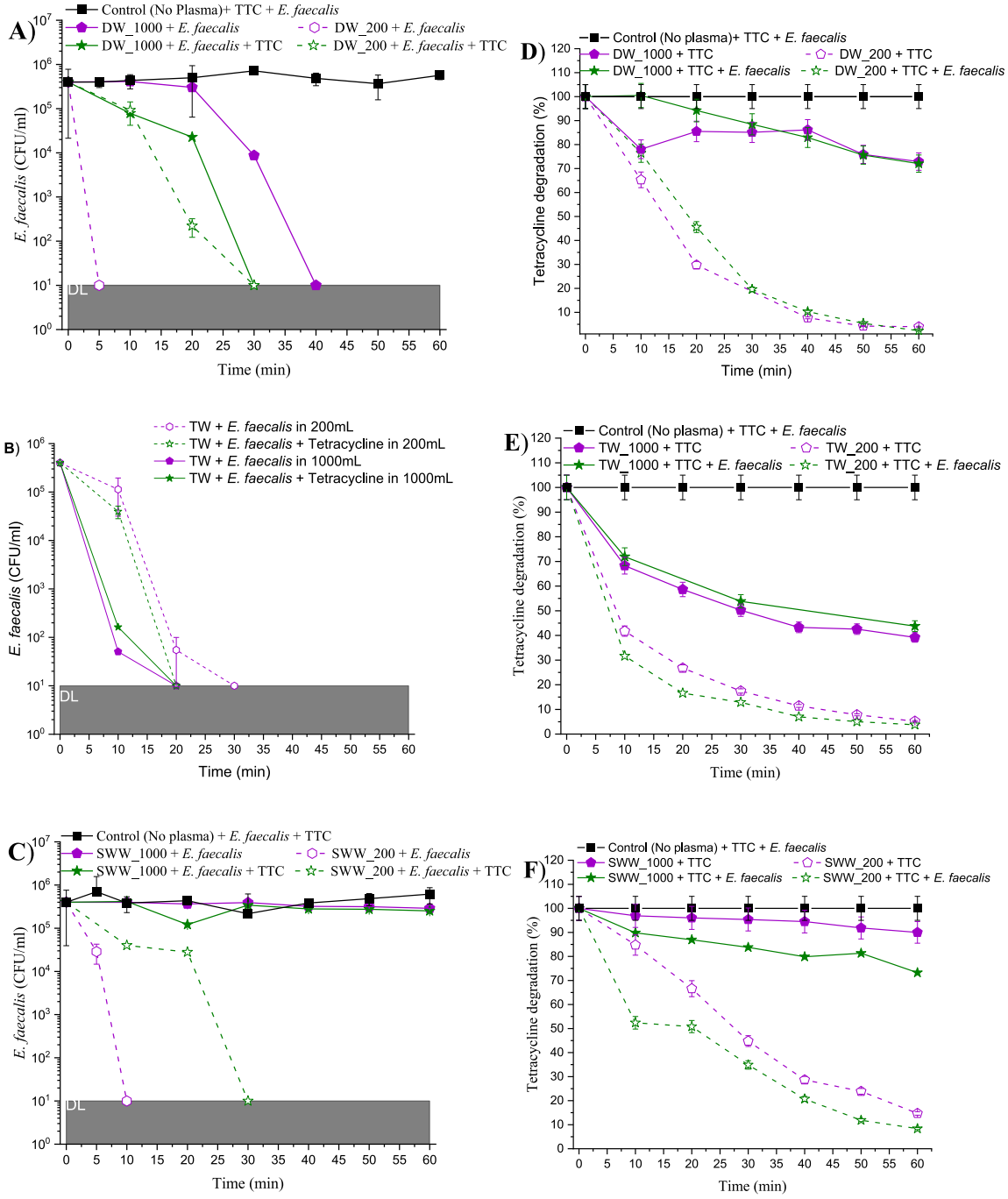

Fig. 5. Pollutant removal efficiency, in the reactor of 200 mL (discontinuous line), in the reactor of 1000 mL (continuous line). Treatment for separate (pink colour) or in combination (green colour). Control (black) in the different aqueous matrices No plasma with tetracycline and *E. faecalis* A) *E. faecalis* inactivation in DW; B) E. faecalis inactivation in TW, C) *E. faecalis* in SWW. D) Tetracycline degradation in DW. E) Tetracycline degradation in TW. F) Tetracycline degradation in SWW.

In Fig. 5D, E, F, tetracycline removal in the different conditions discussed are shown. For the reactor of 200 mL faster rates of tetracycline degradation were achieved, reaching between 90 % and 99 % removal efficiencies in all the aqueous matrices at 60 min of reaction and depicting energy efficiency per order values of 68, 87 and 137 kW/m^3 for DW, TW and SWW, respectively, for single tetracycline pollutant. In the case of tetracycline removal, there was not a significance difference between the presence of one or two contaminants. However, there were differences between reactors. In the reactor of 1000 mL, the removal after one hour of treatment was lower, achieving near 30 % for DW, 50 % for TW and 15 % for SWW. The presence of *E. faecalis* in the reactor did not make a significance difference in the degradation rates of the tetracycline. Once again, the higher degradation rates in TW were due to the activation of the residual chloride coming dissolved in the tap water. Chloride anions in the presence of the plasma generates reactive chlorine and hypochlorite radicals that enhances tetracycline degradation (Fang et al., 2022). Although it is possible to degrade tetracycline with direct plasma technologies, the total mineralization was lower. Only a reduction of 3.1 % of the total organic carbon conversion was observed for DW, 0.8 % for TW, and 12.6 % for SWW. This plasma treatment demonstrates good performance in the removal of tetracycline but lacks sufficient energy input to achieve complete mineralization of the pollutant. Previous works (Wu et al., 2025) with a needle to plane reactor discharge, have achieved 80 % in tetracycline removal

with near an 8 % of mineralization. Other studies (Fang et al., 2022) have achieved 81.5 % removal with air plasma reactor and 96.5 % removal with oxygen plasma reactor. These degradation rates are a bit lower than the ones achieved in this work of near 90–99 % for the 200 mL. Achieving a high mineralization rate is a challenge where plasma technologies are increasing its efficiency along the years.

Macroscopic images of the bacterial colonies can be seen in Supplementary Figure S3. Controls were performed for each aqueous matrix, and 25 ppm of tetracycline and *E. faecalis* were added.

3.5. DBP formation and evaluation

Lastly some inorganic and organic DBPs were analysed. In the Table 2 all the measured DBPs in this work are shown. From the organic DBPs, bromodichloromethane, dibromochloromethane and bromoform have not been detected, being the chloroform the only one observed. With a concentration of 2.22, 2.45 and 2.43 μg/L for DW, TW and SWW in the 200 mL reactor and with a higher appearance in the 1000 mL reactor, showing values of 5.06, 8.62 and 9.51 μg/L for DW, TW and SWW. These values were much lower than the legal maximum (100 μg/L) of potable water for consumption in Spain (Real Decreto 3/2023, 2023). For the inorganic DBPs, mainly the ones derived from chloride and bromide were analysed, not being detected any of them. Previous studies corroborate that non thermal plasmas treatment does not produce dangerous DBPs (Guo et al., 2025). However, bromate was not produced because no bromide was present in the samples before treatment. To evaluate whether this transient spark plasma discharge could produce bromate, bromide-spiked samples were treated with plasma. The results showed an increase in bromate concentration of approximately 1.732 mg/L and a reduction in bromide of 0.973 mg/L. The conversion pathway from bromide to bromate can be represented by Eq. (21) (Morrison et al., 2023). The concentration of bromate is not yet regulated in Spanish wastewater reuse regulations (Real Decreto 1085/2024, 2024). However, drinking water regulations establish a maximum permissible concentration of 10 μg/L (Real Decreto 3/2023, 2023).

$$Br^- \xrightarrow{O_3} OBr/HOBr \xrightarrow{O_3} BrO_2^- \xrightarrow{O_3} BrO_3^- \quad (21)$$

Most of the THMs are generated by reaction of chlorine with the organic matter (Kali et al., 2021). Among the main THMs, chloroform is the most stable, being the one with a higher persistence in the water (Kali et al., 2021), being possible to find it even before the chlorination treatment. Some authors (Gao et al., 2023; Breider and Hunkeler, 2014), have reported the presence of chloroform before the treatment. However, chloroform could have been generated in the samples due to the oxidation of the chloride anion, as previously reported by the authors (Breider and Hunkeler, 2014). The main pathway involves the oxidation of the chloride anion by plasma-generated oxidative species such as ozone, singlet oxygen, or hydroxyl radicals, producing chlorine and hypochlorite radicals. These radicals react with the organic matter dissolved in the water to form chlorinated organic intermediates. This reaction is followed by stepwise halogenation, ultimately producing chloroform. Once formed, chloroform can persist in the medium for long times.

Non-thermal plasma treatments are a good alternative; not only because chlorine is not required for pollutant removal, but also because plasma technologies have the ability to degrade certain THMs. Gao et al. (Gao et al., 2023) evaluated the ability of a plasma bubble discharge system to reduce different DBPs. They also reported initial concentrations of certain THMs such as chloroform being reduced from 16 μg/L to approximately 3 μg/L in one hour of treatment. Morrison et al. (Morrison et al., 2023), reported a 70 % reduction in THMs using a DBD discharge. Sarangapani et al. (Sarangapani et al., 2018) used a plasma treatment achieving a reduction of near 70 % of total THMs concentration after 30 mins of treatment.

Considering previous reports in literature (Guo et al., 2025; Gao et al., 2023; Sarangapani et al., 2018) it is likely that the detected chloroform was not generated during the process, but it was being decomposed and reduced from the one already existing in the water samples. Additionally, in some data not published yet by this research team, there was reached near a 75 % reduction in the total concentration of THMs after one hour with the same plasma treatment in a reactor of 200 mL. It is possible to conclude that this plasma discharge technology not only can remove pollutants in water but also can degrade present DBPs like THMs. While no additional THMs were generated. Considering this, the lower concentration observed in the reactor of 200 mL comparing to the 1000 mL can be explained by the higher degradation of chloroform in the 200 mL reactor as it has been reported along this manuscript.

Lastly, after comparing the chemical production, pollutant removal efficiency, and DBPs formation in both reactors, it is crucial to evaluate the scalability of the technology. This transient spark discharge, characterized by low energy consumption, has proven to be an effective method for pollutant removal without the need for chemical additives and without generating DBPs above regulatory limits. However, the primary limitation of this technology lies in the technical challenges related to scaling up the treated volume. Although it operates with high energy efficiency, the requirement for high voltage and the limitations of power supplies constrain the maximum plasma discharge volume. Scalability could potentially be achieved through continuous-flow treatment modes, processing smaller volumes with treated water storage, but this aspect exceeds the scope of the present study.

4. Conclusions

This work demonstrates that this plasma is a viable technology for water treatment in different water samples compositions. This technology can remove different pollutants from the water and being safe due to low DBPs detection. Only chloroform was detected but in a very low concentration, lower than 2.5 μg/L for the 200 mL reactor and less than 10 μg/L for the 1000 mL reactor for the same treatment time. Chloroform is thought to be removed from the water samples due to the plasma treatment.

The water composition plays a key role in the reaction between RONS altering the concentration in the PAW. The changes in the pH during the plasma treatment also have influence in how those species evolve after the treatment. Additionally, the volume of the reactor for

Table 2
Inorganic and organic DBPs concentrations.

Sample code	[Chloroform], (μg/L)	Bromodichloromethane (μg/L)	Dibromochloromethane (μg/L)	Bromoform (μg/L)	Chlorite (mg/L)	Bromate (mg/L)	Chlorate (mg/L)
DW200	2.220	ND	ND	ND	ND	ND	ND
TW200	2.453	ND	ND	ND	ND	ND	ND
SWW200	2.433	ND	ND	ND	ND	ND	ND
DW1000	5.063	ND	ND	ND	ND	ND	ND
TW1000	8.622	ND	ND	ND	ND	ND	ND
SWW1000	9.516	ND	ND	ND	ND	ND	ND

*ND Non-detected

this type of technology is an important factor. During the treatment the nitrate concentration rises, while the nitrite shows an initial increase followed by a reduction due to the reaction of this specie with hydrogen peroxide to generate nitrate. Ammonium and ozone were also increased during the treatment time, and the hydrogen peroxide had a similar effect than nitrite. After the treatment, in general nitrate and ammonium remained constant for most of the conditions evaluated. Nitrite had slow reduction in most of the samples, being the rate higher for samples with a lower pH value. Lastly, ozone and hydrogen peroxide are highly reactive species; therefore, they were not detected one week after the treatment..

There is a clear influence between chemical species generated in the PAW and the pollutant removal efficiency in the reactor. Lower concentrations of reactive species conduct to lower pollutant removal efficiency. There is a direct impact in the pollutant degradation efficiency and the number of pollutants in the sample. For the degradation of *E. faecalis*, the presence of tetracycline increased the treatment time required for complete depletion of the bacteria, also the energy efficiency per order was increased from 2.14 to 12.34 kW/m^3. So, when there was more than one contaminant in the reactor higher treatment times for same level of pollutant removal, were required. Implying there is a competition between plasma species and the pollutnats removed. Although plasma is a good technology for tetracycline degradation, it is necessary to combine with other technologies for a proper mineralization of the totality of organic matter.

In this study, the main chemical changes were evaluated in different types of water and reactors of different volumes, showing that higher concentrations of reactive species were achieved in the 200 mL reactor. In addition, higher pollutant removal efficiencies were achieved in this reactor. Finally, the capacity of this technology was evaluated not only regarding the absence of THM formation, but also its ability to degrade existing THMs.

CRediT authorship contribution statement

J.I. Quintana-Terriza: Writing – review & editing, Writing – original draft, Visualization, Validation, Methodology, Investigation, Formal analysis, Data curation, Conceptualization. **P. García-Muñoz:** Writing – review & editing, Visualization, Supervision, Resources, Project administration, Funding acquisition, Conceptualization. **M.J. Mena:** Investigation. **M. Zúñiga:** Investigation.

Declaration of Competing Interest

The authors declare that they have no known competing financial interests or personal relationships that could have appeared to influence the work reported in this paper.

Acknowledgements

This research has been supported by CEDRION C.T.I. S.L and the Consejería de Investigación y Educación (Programa de Doctorados Industriales, Comunidad Autónoma de Madrid) through an industrial doctoral proyect (IND2022/AMB-23691) to J.I. Quintana-Terriza. This work has received financial support from Spanish MCIN/AEI/10.13039/501100011033 and "ERDF A way of making Europe", through project PHOTORAS (PID2021–128165OA-I00).

Appendix A. Supporting information

Supplementary data associated with this article can be found in the online version at doi:10.1016/j.psep.2025.108353.

References

Akishev, Y., Grushin, M., Karalnik, V., Petryakov, A., Trushkin, N., 2010. Non-equilibrium constricted dc glow discharge in N2 flow at atmospheric pressure: stable and unstable regimes. J. Phys. D Appl. Phys. 43 (7), 075202. https://doi.org/10.1088/0022-3727/43/7/075202.

Amsalu, K., et al., 2024. Abatement and biotoxicity assessment of chlorpyrifos residue from green coffee beans: effect of non-thermal plasma generated ozone and nitric oxide species. Chem. Eng. J. 497, 154364. https://doi.org/10.1016/J.CEJ.2024.154364.

Anbar, M., 1964. On the sonochemical formation of hydrogen peroxide in water. J. Phys. Chem. 68 (2), 352–355. https://doi.org/10.1021/J100784A025/ASSET/J100784A025.FP.PNG_V03.

Anbar, M., Taube, H., 1954. Interaction of nitrous acid with hydrogen peroxide and with water. J. Am. Chem. Soc. 76 (24), 6243–6247. https://doi.org/10.1021/JA01653A007/ASSET/JA01653A007.FP.PNG_V03.

Andrés, C.M.C., Pérez de la Lastra, J.M., Andrés Juan, C., Plou, F.J., Pérez-Lebeña, E., 2023. Superoxide anion chemistry—its role at the core of the innate immunity. Int. J. Mol. Sci. 24 (3). https://doi.org/10.3390/IJMS24031841.

Behruznia, M., Gordon, D.M., 2022. Molecular and metabolic characteristics of wastewater associated Escherichia coli strains. Environ. Microbiol. Rep. 14 (4), 646–654. https://doi.org/10.1111/1758-2229.13076.

Benson, N.U., Akintokun, O.A., Adedapo, A.E., 2017. Disinfection byproducts in drinking water and evaluation of potential health risks of long-term exposure in Nigeria. J. Environ. Public Health 2017 (1), 7535797. https://doi.org/10.1155/2017/7535797.

Bond, T., Templeton, M.R., Mokhtar Kamal, N.H., Graham, N., Kanda, R., 2015. Nitrogenous disinfection byproducts in English drinking water supply systems: occurrence, bromine substitution and correlation analysis. Water Res. 85, 85–94. https://doi.org/10.1016/J.WATRES.2015.08.015.

Breider, F., Hunkeler, D., 2014. Mechanistic insights into the formation of chloroform from natural organic matter using stable carbon isotope analysis. Geochim Cosmochim. Acta 125, 85–95. https://doi.org/10.1016/J.GCA.2013.09.028.

Bruggeman, P.J., et al., 2016. Plasma-liquid interactions: a review and roadmap. Z. Lj. Petrovic 24 (5). https://doi.org/10.1088/0963-0252/25/5/053002.

Bruggeman, P., Leys, C., 2009. Non-thermal plasmas in and in contact with liquids. J. Phys. D Appl. Phys. 42 (5), 053001. https://doi.org/10.1088/0022-3727/42/5/053001.

Calvo, T., Prieto, M., Alvarez-Ordóñez, A., López, M., 2020. Effect of non-thermal atmospheric plasma on food-borne bacterial pathogens on ready-to eat foods: morphological and physico-chemical changes occurring on the cellular envelopes. Foods 9 (12). https://doi.org/10.3390/foods9121865.

Eisenberg, G.M., 1943. Colorimetric determination of hydrogen peroxide. Philadelphia. https://doi.org/10.1021/i560117a011.

Fang, C., Wang, S., Xu, H., Huang, Q., 2022. Degradation of tetracycline by atmospheric-pressure non-thermal plasma: enhanced performance, degradation mechanism, and toxicity evaluation. Sci. Total Environ. 812. https://doi.org/10.1016/J.SCITOTENV.2021.152455.

Gao, X., Wang, X., Ma, J., Liu, Y., 2023. Potential and mechanism of disinfection by-products removal in drinking water by bubbling corona discharge. Water Res 245, 120624. https://doi.org/10.1016/j.watres.2023.120624.

Grellier, J., Rushton, L., Briggs, D.J., Nieuwenhuijsen, M.J., 2015. Assessing the human health impacts of exposure to disinfection by-products — a critical review of concepts and methods. Environ. Int 78, 61–81. https://doi.org/10.1016/J.ENVINT.2015.02.003.

Guerra-Rodríguez, S., et al., 2023. Pilot-scale sulfate radical-based advanced oxidation for wastewater reuse: simultaneous disinfection, removal of contaminants of emerging concern, and antibiotic resistance genes. Chem. Eng. J. 477, 146916. https://doi.org/10.1016/j.cej.2023.146916.

Guo, X., et al., 2015. Common oxidants activate the reactivity of zero-valent iron (ZVI) and hence remarkably enhance nitrate reduction from water. Sep Purif. Technol. 146, 227–234. https://doi.org/10.1016/J.SEPPUR.2015.03.059.

Guo, H., Wang, Y., Wang, J., Tang, S., Wang, T., 2025. Review on application of non-thermal plasma for disinfection: direct plasma and indirect plasma-activated water. Chin. Chem. Lett., 111275 https://doi.org/10.1016/J.CCLET.2025.111275.

Hao, O.J., 2003. Part 3: microbiology of wastewater treatment. Handb. Water Wastewater Microbiol. 459–469. Accessed: Jun. 23, 2025. [Online]. Available: ⟨http://www.sciencedirect.com/science/article/pii/B9780124701007500297⟩.

S. Ikawa, K. Kitano, and S. Hamaguchi, "Effects of pH on Bacterial Inactivation in Aqueous Solutions due to Low-Temperature Atmospheric Pressure Plasma Application," 2010, doi: 10.1002/ppap.200900090.

Janda, M., 2011. Transient spark. Control Electr. Circuit Parameters. https://doi.org/10.1088/0963-0252/20/3/035015.

Jang, J., Hur, H.G., Sadowsky, M.J., Byappanahalli, M.N., Yan, T., Ishii, S., 2017. Environmental Escherichia coli: ecology and public health implications—a review. J. Appl. Microbiol. 123 (3), 570–581. https://doi.org/10.1111/JAM.13468.

Kali, S., et al., 2021. Occurrence, influencing factors, toxicity, regulations, and abatement approaches for disinfection by-products in chlorinated drinking water: a comprehensive review (Jul.). Environ. Pollut. 281, 116950. https://doi.org/10.1016/J.ENVPOL.2021.116950 (Jul.).

Kalita, I., Kamilaris, A., Havinga, P., Reva, I., 2024. Assessing the health impact of disinfection byproducts in drinking water. ACS Est. Water 4 (4), 1564. https://doi.org/10.1021/ACSESTWATER.3C00664.

Khadre, M.A., Yousef, A.E., Kim, J.G., 2001. Microbiological aspects of ozone applications in food: a review. J. Food Sci. 66 (9), 1242–1252. https://doi.org/10.1111/J.1365-2621.2001.TB15196.X.

Khlyustova, A., Labay, C., Machala, Z., Ginebra, M.-P., Canal, C., 2019. Important parameters in plasma jets for the production of RONS in liquids for plasma medicine: a brief review. Springe Nat. https://doi.org/10.1007/s11705-019-1801-8.
Kimura, S.Y., Ortega-Hernandez, A., 2019. Formation mechanisms of disinfection byproducts: recent developments. Curr. Opin. Environ. Sci. Health 7, 61–68. https://doi.org/10.1016/J.COESH.2018.11.002.
Komarudin, A.G., Nei, D., Kameya, H., Sotome, I., Araki, T., 2023. Characterization of a non-thermal plasma-bubbling system as a novel sanitizer: physicochemical properties, bactericidal effect, and reactive species. Food Sci. Technol. Res 29 (5), 365–376. https://doi.org/10.3136/fstr.FSTR-D-23-00011.
Kooshki, S., Pareek, P., Janda, M., Machala, Z., 2024. Selective reactive oxygen and nitrogen species production in plasma-activated water via dielectric barrier discharge reactor: an innovative method for tuning and its impact on dye degradation. J. Water Process Eng. 63, 105477. https://doi.org/10.1016/J.JWPE.2024.105477.
Krasner, S.W., Mitch, W.A., McCurry, D.L., Hanigan, D., Westerhoff, P., 2013. Formation, precursors, control, and occurrence of nitrosamines in drinking water: a review. Water Res 47 (13), 4433–4450. https://doi.org/10.1016/J.WATRES.2013.04.050.
Lee, G.J., et al., 2021. Nitrate capture investigation in plasma-activated water and its antifungal effect on cryptococcus pseudolongus cells. Int J. Mol. Sci. 22 (23). https://doi.org/10.3390/IJMS222312773.
Liu, F., et al., 2010. Inactivation of bacteria in an aqueous environment by a direct-current, cold-atmospheric-pressure air plasma microjet. Plasma Process. Polym. 7 (3–4), 231–236. https://doi.org/10.1002/PPAP.200900070.
Lou, J., Wang, W., Zhu, L., 2021. Transformation of emerging disinfection byproducts Halobenzoquinones to haloacetic acids during chlorination of drinking water. Chem. Eng. J. 418, 129326. https://doi.org/10.1016/J.CEJ.2021.129326.
Lukes, P., Dolezalova, E., Sisrova, I., Clupek, M., 2014. Aqueous-phase chemistry and bactericidal effects from an air discharge plasma in contact with water: evidence for the formation of peroxynitrite through a pseudo-second-order post-discharge reaction of H 2 O 2 and HNO. Plasma Sources Sci. Technol. 16. https://doi.org/10.1088/0963-0252/23/1/015019.
Ma, S., Kim, K., Chun, S., Moon, S.Y., Hong, Y., 2020. Plasma-assisted advanced oxidation process by a multi-hole dielectric barrier discharge in water and its application to wastewater treatment. Chemosphere 243. https://doi.org/10.1016/J.CHEMOSPHERE.2019.125377.
Ma, S., Kim, K., Huh, J., Hong, Y., 2017. Characteristics of microdischarge plasma jet in water and its application to water purification by bacterial inactivation. Sep Purif. Technol. 188, 147–154. https://doi.org/10.1016/J.SEPPUR.2017.07.034.
Machala, Z., Tarabova, B., Hensel, K., Spetlikova, E., Sikurova, L., Lukes, P., 2013. Formation of ROS and RNS in water electro-sprayed through transient spark discharge in air and their bactericidal effects (Jul.). Plasma Process. Polym. 10 (7), 649–659. https://doi.org/10.1002/PPAP.201200113 (Jul.).
Maniruzzaman, M., et al., 2017. Nitrate and hydrogen peroxide generated in water by electrical discharges stimulate wheat seedling growth. Plasma Chem. Plasma Process. 37, 1393–1404. https://doi.org/10.1007/s11090-017-9827-5.
McCarthy, J.E.M., Hynds, P.D., Bolton, D.J., Celayeta, J.M.F., 2025. Prevalence and concentrations of four waste-pathogen combinations from land-spreading across high-income, temperate regions: meta-modelling and distribution fitting for quantitative microbial risk assessment (QMRA). Micro Risk Anal., 100348 https://doi.org/10.1016/J.MRAN.2025.100348.
Meropoulis, S., Aggelopoulos, C.A., 2023. Plasma microbubbles vs gas-liquid DBD energized by low-frequency high voltage nanopulses for pollutants degradation in water: destruction mechanisms, composition of plasma-activated water and energy assessment. J. Environ. Chem. Eng. 11 (3), 109855. https://doi.org/10.1016/J.JECE.2023.109855.
Morrison, C.M., et al., 2023. CriticaL Review on Bromate Formation during Ozonation and Control Options for Its Minimization. Environ. Sci. Technol. 57 (47), 18393–18409. https://doi.org/10.1021/ACS.EST.3C00538.
Morrison, C.M., Hogard, S., Pearce, R., Gerrity, D., von Gunten, U., Wert, E.C., 2022. Ozone disinfection of waterborne pathogens and their surrogates: a critical review. Water Res 214, 118206. https://doi.org/10.1016/J.WATRES.2022.118206.
Naítali, M., Kamgang-Youbi, G., Herry, J.M., Bellon-Fontaine, M.N., Brisset, J.L., 2010. Combined Effects of Long-Living Chemical Species during Microbial Inactivation Using Atmospheric Plasma-Treated Water. Appl. Environ. Microbiol 76 (22), 7662–7664. https://doi.org/10.1128/AEM.01615-10.
Nathanael, R.J., Adyanis, L.N., Oginawati, K., 2024. The last decade epidemiologic concern of drinking water contaminants of emerging concern (CECs) in Asian Countries: a scoping review. Heliyon 10 (20), e39236. https://doi.org/10.1016/J.HELIYON.2024.E39236.
D. Panchal, Q. Lu, K. Sakaushi, and X. Zhang, "Advanced cold plasma-assisted technology for green and sustainable ammonia synthesis," 2024, doi: 10.1016/j.cej.2024.154920.
Pandis, P.K., et al., 2022. Key points of advanced oxidation processes (AOPs) for wastewater, organic pollutants and pharmaceutical waste treatment: a mini review. ChemEngineering 6 (1), 8. https://doi.org/10.3390/CHEMENGINEERING6010008.
Papalexopoulou, K., Triantaphyllidou, I.E., Skandalis, S.S., Rassias, G., Aggelopoulos, C. A., 2025. Optimization of pulsed DBD plasmas for the degradation of Valsartan in water – application to pharmaceutical pollutants of other molecular classes (Jul.). Chem. Eng. J. 515, 163732. https://doi.org/10.1016/J.CEJ.2025.163732 (Jul.).
S. Perinban, V. Orsat, and V. Raghavan, "Nonthermal Plasma-Liquid Interactions in Food Processing: A Review," 2019, doi: 10.1111/1541-4337.12503.
Polo-López, M.I., et al., 2012. Mild solar photo-Fenton: An effective tool for the removal of Fusarium from simulated municipal effluents. Appl. Catal. B 111–112, 545–554. https://doi.org/10.1016/J.APCATB.2011.11.006.
Postigo, C., et al., 2021. A step forward in the detection of byproducts of anthropogenic organic micropollutants in chlorinated water. Trends Environ. Anal. Chem. 32, e00148. https://doi.org/10.1016/J.TEAC.2021.E00148.
Qadafi, M., Rosmalina, R.T., Pitoi, M.M., Wulan, D.R., 2023. Chlorination disinfection by-products in Southeast Asia: A review on potential precursor, formation, toxicity assessment, and removal technologies. Chemosphere 316, 137817. https://doi.org/10.1016/J.CHEMOSPHERE.2023.137817.
Quintana-Terriza, J.I., Fernández-García, C., García-Muñoz, P., Rodríguez-Chueca, J., 2025. Dual action of plasma discharge: E. faecalis inactivation and tetracycline degradation with eco-safe effluents. Water Res X 29, 100429. https://doi.org/10.1016/J.WROA.2025.100429.
Real Decreto 3/2023, de 10 de enero, por el que se establecen los criterios técnico-sanitarios de la calidad del agua de consumo, su control y suministro." Accessed: Dec. 02, 2025. [Online]. Available: ⟨https://www.boe.es/eli/es/rd/2023/01/10/3/con⟩.
Real Decreto 1085/2024, de 22 de octubre, por el que se aprueba el Reglamento de reutilización del agua y se modifican diversos reales decretos que regulan la gestión del agua. 2024. Accessed: Dec. 30, 2024. [Online]. Available: ⟨https://www.boe.es⟩.
REGULATION (EU) 2020/741 of the European Parliament and of the Council of 25 May 2020 on minimum requirements for water reuse (Text with EEA relevance)."
Ren, H.T., Jia, S.Y., Zou, J.J., Wu, S.H., Han, X., 2015. A facile preparation of Ag2O/P25 photocatalyst for selective reduction of nitrate. Appl. Catal. B 176–177, 53–61. https://doi.org/10.1016/j.apcatb.2015.03.038.
Rezaei, F., Vanraes, P., Nikiforov, A., Morent, R., De Geyter, N., 2019. Applications of plasma-liquid systems: a review. Materials 12 (7). https://doi.org/10.3390/MA12172751.
Rocha, R.S., Nogueira, B., Souto, R.S., Lanza, M.R.V., Rodrigo, M.A., 2025. New insights on efficient electrochemical production of hydrogen peroxide. Electrochim. Acta, 146546. https://doi.org/10.1016/J.ELECTACTA.2025.146546.
Sarangapani, C., Lu, P., Behan, P., Bourke, P., Cullen, P.J., 2018. Humic acid and trihalomethane breakdown with potential by-product formations for atmospheric air plasma water treatment. J. Ind. Eng. Chem. 59, 350–361. https://doi.org/10.1016/J.JIEC.2017.10.042.
Schuchert-Shi, A., Hauser, P.C., 2008. Monitoring the enzymatic conversion of urea to ammonium by conventional or microchip capillary electrophoresis with contactless conductivity detection. Anal. Biochem 376 (2), 262–267. https://doi.org/10.1016/J.AB.2008.02.030.
Shi, J., et al., 2024. Exposure to disinfection by-products and risk of cancer: A systematic review and dose-response meta-analysis. Ecotoxicol. Environ. Saf. 270, 115925. https://doi.org/10.1016/J.ECOENV.2023.115925.
Smith, H.V., Grimason, A.M., 2003. Giardia and cryptosporidium in water and wastewater. Handb. Water Wastewater Microbiol. 695–756. https://doi.org/10.1016/B978-012470100-7/50041-8.
Thirumdas, R., et al., 2018. Plasma activated water (PAW): Chemistry, physico-chemical properties, applications in food and agriculture. Trends Food Sci. Technol. 77 (September 2017), 21–31. https://doi.org/10.1016/j.tifs.2018.05.007.
Triantaphyllidou, I.E., Aggelopoulos, C.A., 2025. Insights on bacteria inactivation in water by cold plasma: Effect of water matrix and pulsed plasmas waveform on physicochemical water properties, species formation and inactivation efficiency of Escherichia coli. Environ. Res. 266, 120467. https://doi.org/10.1016/J.ENVRES.2024.120467.
United Nations Educational Scientific and Cultural Organization, 2021. The United Nations World Water Development Report 2021: Valuing water. Water Politics, p. 206. ⟨https://unesdoc.unesco.org/ark:/48223/pf0000375724⟩. Accessed: Jan. 04, 2024. [Online]. Available:
Van Gils, C.A.J., Hofmann, S., Boekema, B.K.H.L., Brandenburg, R., Bruggeman, P.J., 2013. Mechanisms of bacterial inactivation in the liquid phase induced by a remote RF cold atmospheric pressure plasma jet. J. Phys. D. Appl. Phys. 46 (17), 175203. https://doi.org/10.1088/0022-3727/46/17/175203.
Von Gunten, U., 2003. Ozonation of drinking water: Part I. Oxidation kinetics and product formation. Water Res 37 (7), 1443–1467. https://doi.org/10.1016/S0043-1354(02)00457-8.
Wang, Z., et al., 2022. Combination of NOxmode and O3mode air discharges for water activation to produce a potent disinfectant. Plasma Sources Sci. Technol. 31 (5). https://doi.org/10.1088/1361-6595/AC60C0.
Wang, L., et al., 2025. Health risk assessment via ingestion of disinfection by-products in drinking water. Sci. Rep. 15 (1), 1793. https://doi.org/10.1038/s41598-024-84094-9.
Wang, C., He, T., Zhang, M., Zheng, C., Yang, L., Yang, L., 2024. Review of the mechanisms involved in dissimilatory nitrate reduction to ammonium and the efficacies of these mechanisms in the environment. Environ. Pollut. 345, 123480. https://doi.org/10.1016/J.ENVPOL.2024.123480.
Wei, C., Zhang, F., Hu, Y., Feng, C., Wu, H., 2017. Ozonation in water treatment: the generation, basic properties of ozone and its practical application. Rev. Chem. Eng. 33 (1), 49–89. https://doi.org/10.1515/REVCE-2016-0008.
Wong, K.S., Chew, N.S.L., Low, M., Tan, M.K., 2023. Plasma-Activated Water: Physicochemical Properties, Generation Techniques, and Applications (Jul.). Processes 11 (7), 2213. https://doi.org/10.3390/pr11072213 (Jul.).
Wu, H., Ye, W., Shen, W., Zhao, Q., 2025. Tetracycline degradation in the system of peracetic acid activation by liquid discharge plasma. Sep Purif. Technol. 354, 128783. https://doi.org/10.1016/j.seppur.2024.128783.
Xu, M., et al., 2021. Synergistic effects of UVC and oxidants (PS vs. Chlorine) on carbamazepine attenuation: Mechanism, pathways, DBPs yield and toxicity assessment. Chem. Eng. J. 413, 127533. https://doi.org/10.1016/J.CEJ.2020.127533.

Yang, L., Zhang, Z., Chen, Z., 2021. Formation of nitrite and ammonium during the irradiation of nitrate-containing water by VUV/UV. J. Water Process Eng. 40, 101801. https://doi.org/10.1016/J.JWPE.2020.101801.

Z.C. Liu, D. X .Liu, C .Chen, D. Li, A. J. Yang, M. Z. Rong, H. L. Chen and M. G. Kong, "Physicochemical Processes in the Indirect Interaction between Surface Air Plasma and Deionized Water," 2015, doi: 10.1088/0022-3727/48/49/495201.

W. Zhang *et al.*, "Reactor Structural Parameters Effect on the Degradation of o-Dichlorobenzene under DBD-NTP System," 2023, doi: 10.1061/JOEEDU.EEENG-7416.

Zhang, Y.S., et al., 2025. Enhanced peroxone reaction with amphoteric oxide modulation for efficient decontamination of challenging wastewaters: comparative performance, economic evaluation, and pilot-scale implementation. Water Res. 274, 123058. https://doi.org/10.1016/J.WATRES.2024.123058.

Zhao, Y.M., Patange, A., Sun, D.W., Tiwari, B., 2020. Plasma-activated water: physicochemical properties, microbial inactivation mechanisms, factors influencing antimicrobial effectiveness, and applications in the food industry. Compr. Rev. Food Sci. Food Saf. 19 (6), 3951–3979. https://doi.org/10.1111/1541-4337.12644.

Y. Zhong, Z. Jin, M. Chen, and Z. Yang, "An experimental investigation of the thermal effects in AC-DBD plasma actuator on the melting process of an ice bead," 2023, doi: 10.1016/j.expthermflusci.2023.110950.

Zoumpouli, G.A., Siqueira Souza, F., Petrie, B., Féris, L.A., Kasprzyk-Hordern, B., Wenk, J., 2020. Simultaneous ozonation of 90 organic micropollutants including illicit drugs and their metabolites in different water matrices. Environ. Sci. (Camb.) 6 (9), 2465–2478. https://doi.org/10.1039/D0EW00260G.

Zumft, W.G., 1997. Cell biology and molecular basis of denitrification. Microbiol. Mol. Biol. Rev. 61 (4), 533–616. https://doi.org/10.1128/MMBR.61.4.533-616.1997.